ChemPubSoc Europe

DOI: 10.1002/cmdc.201402558

CHEMMEDCHEM Full Papers

P2-Quinazolinones and Bis-Macrocycles as New Templates for Next-Generation Hepatitis C Virus NS3/4a Protease Inhibitors: Discovery of MK-2748 and MK-6325

Michael T. Rudd,*[a] John W. Butcher,[a] Kevin T. Nguyen,[a] Charles J. McIntyre,[a] Joseph J. Romano,[a] Kevin F. Gilbert,[a] Kimberly J. Bush,[a] Nigel J. Liverton,[a] M. Katharine Holloway,[b] Steven Harper,[c] Marco Ferrara,[c] Marcello DiFilippo,[c] Vincenzo Summa,[c] John Swestock,[d] Jeff Fritzen,[d] Steven S. Carroll,[e] Christine Burlein,[e] Jillian M. DiMuzio,[e] Adam Gates,[e] Donald J. Graham,[e] Qian Huang,[e] Stephanie McClain,[e] Carolyn McHale,[e] Mark W. Stahlhut,[e] Stuart Black,[f] Robert Chase,[f] Aileen Soriano,[f] Christine M. Fandozzi,[g] Anne Taylor,[g] Nicole Trainor,[g] David B. Olsen,[e] Paul J. Coleman,[a] Steven W. Ludmerer,[e] and John A. McCauley*[a]

With the goal of identifying inhibitors of hepatitis C virus (HCV) NS3/4a protease that are potent against a wide range of genotypes and clinically relevant mutant viruses, several subseries of macrocycles were investigated based on observations made during the discovery of MK-5172. Quinazolinone-containing macrocycles were identified as promising leads, and optimization for superior cross-genotype and mutant enzyme potency as well as rat liver and plasma concentrations following oral dosing, led to the development of MK-2748. Additional investigation of a series of bis-macrocycles containing a fused 18- and 15-membered ring system were also optimized for the same properties, leading to the discovery of MK-6325. Both compounds display the broad genotype and mutant potency necessary for clinical development as next-generation HCV NS3/4a protease inhibitors.

Introduction

The leading indication for liver transplantation,[1] hepatitis C is a chronic infection caused by the hepatitis C virus (HCV), which replicates primarily in the liver and is estimated to affect approximately 3% of the world's population with 3–4 million new infections per year.[2] Six major genotypes (gt) of HCV have been identified, with gt1, gt2, and gt3 representing more than 90% of the infections in the developed world. Within genotypes, the virus also displays a high degree of genetic heterogeneity. Although HCV has been treated since the late 1990s[3] with a regimen of co-dosed PEGylated interferon-α (IFN-α) and ribavirin[4] that lasts for up to one year, severe side effects[5] and moderate efficacy have limited the utility of this treatment. Efforts to improve this regimen include development of direct antivirals that inhibit key steps in the viral replication process, and significant progress has been made on this front over the past several years.[6] One major focus of research has been the inhibition of HCV NS3/4a protease,[7,8] a serine protease critical for viral replication. Clinical proof-of-concept was initially established by researchers at Boehringer Ingelheim with BILN-2061.[9] Subsequently, Vertex (VX-950, telaprevir[10]), Merck (SCH-503034, boceprevir;[11] MK-7009, vaniprevir[12–14]) and Johnson & Jonson (simeprevir[15]) have gained

[a] Dr. M. T. Rudd, J. W. Butcher, K. T. Nguyen, C. J. McIntyre, J. J. Romano, K. F. Gilbert, K. J. Bush, Dr. N. J. Liverton, Dr. P. J. Coleman, Dr. J. A. McCauley
Department of Medicinal Chemistry
Merck Research Laboratories, West Point, PA (USA)
E-mail: michael_rudd@merck.com
john_mccauley@merck.com

[b] Dr. M. K. Holloway
Department of Chemistry, Modeling and Informatics
Merck Research Laboratories, West Point, PA (USA)

[c] Dr. S. Harper, Dr. M. Ferrara, Dr. M. DiFilippo, Dr. V. Summa
Department of Medicinal Chemistry
Merck Research Laboratories, Rome (Italy)

[d] J. Swestock, J. Fritzen
Department of Discovery Process Chemistry
Merck Research Laboratories, West Point, PA (USA)

[e] Dr. S. S. Carroll, C. Burlein, J. M. DiMuzio, A. Gates, D. J. Graham, Q. Huang, S. McClain, C. McHale, M. W. Stahlhut, Dr. D. B. Olsen, Dr. S. W. Ludmerer
Department of Antiviral Research
Merck Research Laboratories, West Point, PA (USA)

[f] S. Black, R. Chase, A. Soriano
Department of Antiviral Research
Merck Research Laboratories, Kenilworth, NJ (USA)

[g] Dr. C. M. Fandozzi, A. Taylor, N. Trainor
Department of Drug Metabolism
Merck Research Laboratories, West Point, PA (USA)

Supporting information for this article is available on the WWW under http://dx.doi.org/10.1002/cmdc.201402558.

regulatory approval for HCV NS3/4a inhibitors that are dosed in combination with IFN and ribavirin; these lead to improvements in sustained virological response (SVR) rates. Several other antiviral mechanisms have also been aggressively pursued, and Gilead recently obtained approval for an NS5B polymerase inhibitor (sofusbuvir[16]), which is a key component of the currently recommended treatment for many genotypes. Even with these options available to patients, there remains a compelling need for new oral agents with improved efficacy and tolerability for use as part of all-oral IFN-free combinations containing drugs that target several different mechanisms of action.

As has been detailed in several previous publications, Merck's molecular-modeling-derived strategy was inspired by BILN-2061, but resulted in the development of an alternative[17] macrocyclic core containing a novel P2–P4 linkage; this subsequently led to the discovery of vaniprevir[12,13] and the next-generation NS3/4a protease inhibitor MK-5172 (Figure 1).[18,19] MK-5172, in combination with the NS5A inhibitor MK-8742,[20] recently demonstrated impressive clinical results, received "breakthrough therapy" designation from the US Food and Drug Administration (FDA),[21] and is currently in phase III clinical development.

In the continued pursuit of additional compounds with next-generation profiles similar to that of MK-5172, we decided to follow up on two previously disclosed observations. First, during the development of the P2–P4 macrocyclic series leading ultimately to MK-5172, we discovered the gt3a-potency-enhancing effect of P2-quinoxalines or quinolines with a heteroatom at the 1-position (red 'X' in Figure 1).[19] In contrast to heterocycles that lack this feature, rings with a nitrogen atom at this position had a higher level of broad genotype and mutant enzyme activity, and we wanted to explore the generality of this observation by preparing novel P2 groups that also present a heteroatom in this region (red 'X–Y' in Figure 1). Second, in 2008 we reported the effects of combining P1–P3 and P2–P4 macrocycles to form fused 18-/15-membered bis-macrocycles.[22] With the clinical success of MK-5172, we were also interested to examine the effects of this type of ring system within the context of more optimized P2 and P4 groups. Herein we describe the discovery of two additional next-generation HCV NS3/4a protease inhibitors containing a novel P2-quinazolinone and bis-macrocyclic ring system as the key structural features.

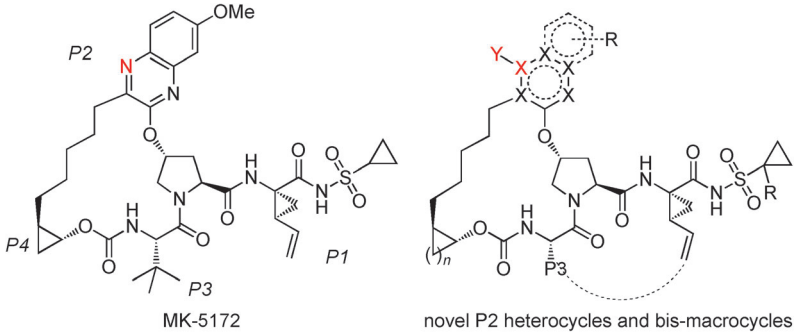

Figure 1. Structure of MK-5172 and general structure for new P2-heterocycles and bis-macrocycles.

Results and Discussion

One of the most important features of the P2–P4 macrocyclic class of HCV NS3/4a protease inhibitors is the P2-heterocycle. Tremendous structural diversity is *tolerated* in this region, but the specific identity of this group is critical to the broad genotype and mutant profile of next-generation inhibitors. As was demonstrated with the publication of the X-ray crystal structure of several inhibitors bound in the NS3/4a active site,[23] the identity of the P2-heterocycle has a significant impact on the binding mode, and is likely responsible for the ability of MK-5172 to maintain high affinity for the clinically important gt1a mutant R155K. As is apparent in Figure 2A, this crystal structure also reveals the possibility of an ordered water molecule interacting with the 1-position nitrogen atom of the quinoxaline ring system. Although this type of water-mediated hydrogen bonding interaction has not been demonstrated in other genotypes or mutant enzymes, it could be partly responsible for the empirically observed increase in potency realized with quinoxalines and 3-oxoquinolines relative to the isomeric 2-oxoquinolines.[19]

Prior to publication of the crystal structure, we did not have an understanding of the effects that lead to the increased potency observed with the P2-quinoxaline (and inclusion of the 1-position nitrogen atom in particular), and therefore we decided to examine this phenomenon further by preparing additional P2-heterocycles containing acceptor groups at this position of the heterocyclic ring (Table 1). Entry **1** shows the baseline level of potency across our standard first-tier assays [gt1b, gt3a, and gt1b mutants (R155K,[24] A156T, A156V, D168Y)] for a simple unsubstituted P2-quinoxaline. Extension of the hydrogen bond acceptor site by one atom results in quinoline *N*-oxide **2**, which is nearly sevenfold *more* potent against gt3a and maintains potency against the rest of the panel, indicating that an acceptor atom external to the ring could be beneficial. Poor oral exposure in rat pharmacokinetics (PK) experiments limited the advancement of quinoline *N*-oxides, but further increased our interest in pursuing related analogues. Replacement of the N–O bond with a 4-hydroxyquinoline C–OH bond (in **3**) maintained good gt3a potency similar to that of quinoxaline **1** and also led to a flattening of the gt1b A156T/V potency in contrast to the more typical two- to threefold shift. Conversion into the 4-methoxyquinoline **4** led to a near 10-fold loss in gt3a potency, whereas introduction of a carbonyl group at this position (entries **5**–**8**) led to sub-nanomolar gt3a potency regardless of the specific heterocycle identity. Figure 2B shows an overlay of a model of isoquinolinone **5** and the X-ray structure of MK-5172 in the gt1a R155K active site, again indicating the possibility of a direct or water-mediated hydrogen bonding interaction with residue 155. Changing the angle of the acceptor atom

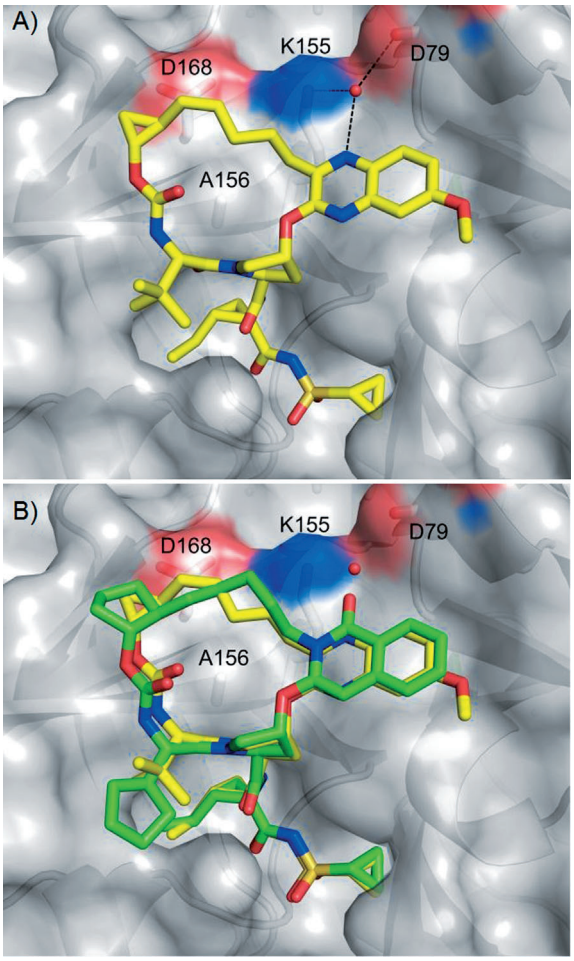

Figure 2. A) X-ray crystal structure of MK-5172 in gt1a R155K showing ordered water and possible hydrogen bonding interactions. B) Model overlay of isoquinolinone **5** (green carbon scaffold) on the structure of MK-5172 shown in panel A.

by introduction of a sulfonyl group (in **9**) led to a significant loss in potency against gt3a and the gt1b mutants. Lastly, removal of the fused phenyl ring (in **10**) or shifting it to a bi-aryl (in **11**) decreased potency five- to tenfold against both gt3a and gt1b mutant enzymes. Following the identification of several novel P2-heterocycles with the potential for next-generation pan-genotype profiles and initial PK profiling (data not shown), we decided to pursue further optimization of the quinazolinone **6**.

As we have discussed in several previous communications,[12,17,19] the plasma PK and oral bioavailability for HCV protease compounds can appear poor, despite high and sustained liver concentrations; this is partially attributed to liver uptake transport, such as organic anion transporting polypeptides (OATPs). Because HCV replicates predominantly in the liver, liver concentrations might be considered a primary driver for efficacy.[25] Therefore, compounds were optimized for high liver concentrations in preclinical species as part of the preliminary PK evaluation. The initial PK assessment measured rat plasma exposure (AUC_{0-4h}) in addition to terminal liver concentrations at 4 h following a 5 mg kg^{-1} oral dose. This strategy has been successful in identifying compounds that also show high liver concentrations in other preclinical species, and was used to identify both MK-5172 and vaniprevir. The ability to obtain good systemic exposure in addition to liver exposure might have an additional advantage, given some evidence for extrahepatic replication sites,[25] and was the strategy behind the discovery of the HCV NS3/4a protease inhibitor MK-1220.[25] Additional HCV NS3/4s protease inhibitor discovery efforts also pursued this more balanced approach of optimizing for compounds with both high preclinical liver and plasma exposures.

Further profiling (Table 2) of initial P2-quinazolinone lead **6** revealed a compound with excellent cellular activity (gt1b replicon $EC_{50}=3$ nM), a small threefold shift in the presence of 50% NHS ($EC_{50}=9$ nM), and good rat liver exposure following p.o. dosing (5 mg kg^{-1} $[liver]_{4h}=9$ μM), which is similar to the level obtained with vaniprevir under the same conditions.[12] Unfortunately, the plasma exposure at this dose was quite low (0.04 μM h), and with additional analogues, the focus was in optimizing for potency as well as rat liver and plasma exposure. As we demonstrated earlier,[19,26] substituents on the P2-heterocycle can have significant effects on potency as well as rat PK. Introduction of a 7-methoxy group (in **12**), which corresponds to the same relative position as the methoxy group in MK-5172, did not significantly improve either enzymatic or cellular potency, and while the rat liver concentration at 4 h was increased more than fourfold following a 5 mg kg^{-1} oral dose, the rat plasma exposure was slightly lower (0.01 μM h). Movement of the methoxy group to the 8-position (in **13**) slightly improved gt1b A156 mutant potency relative to **12**; however, the rat liver concentration at 4 h fell nearly sevenfold, whereas plasma exposure did not increase significantly. Other quinazolinone substituents and cyclic linker constraints were screened, but without appreciable benefit to potency or rat plasma and liver exposure relative to **6** and **12**. For example, **14**, containing a 7-chloroquinazolinone P2 and a methylcyclopropyl carbamate in the linker region, maintained or slightly improved enzymatic potency, but had poor rat liver and plasma exposure. In contrast to the small effects of substituents on the quinazolinone, the introduction of a methyl group into the cyclopropyl acylsulfonamide[27,28] improved plasma exposure dramatically. In comparison with **12**, methylated analogue **15** led to a 70-fold improvement in rat plasma AUC_{0-4h}. Given the excellent broad enzymatic potency, good cellular activity, and promising initial rat PK profile, **15** (MK-2748) was selected for additional profiling.

A more detailed PK study (Table 3) shows **15** to have a high clearance (Cl_p) and moderate volume of distribution (V_d) in rat, whereas it has low Cl_p and V_d values in dog. In both species, **15** has moderate bioavailability (~40% in rat, 27% in dog at 5 and 3 mg kg^{-1}, respectively). In rat, the liver concentrations are maintained at a high level for extended periods. Following a 5 mg kg^{-1} dose of the potassium salt of **15**, the rat liver concentration at 24 h is 28.9 μM, whereas plasma concentrations are 0.017 μM, leading to a liver/plasma ratio ([L]/[P]) of 1700 at 24 h. Relative to the 50% NHS gt1b replicon EC_{50} value (11 nM), liver concentration is maintained at >2600-fold excess out to 24 h. The dog liver concentration (0.28 μM) of **15** was

Table 1. Identification of P2-quinazolinones.

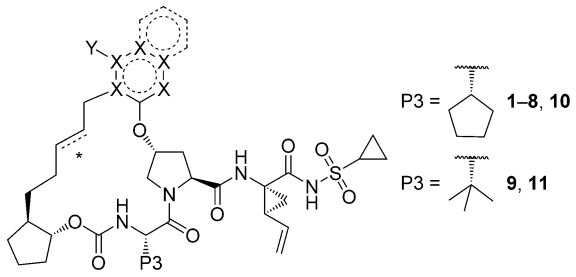

No.	P2-Heterocycle	*Bond	Enzyme Inhibition K_i [nM][a] 1b	3a	R155K	A156T	A156V	D168Y
1	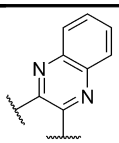	single	$<0.02\pm0$	2.7 ± 0.57	0.16 ± 0	2.7 ± 0.28	8.2 ± 1.8	1.7[b]
2	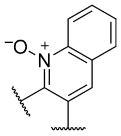	single	0.02 ± 0.01	0.4 ± 0.12	0.06 ± 0.02	1.9 ± 0.2	6.6[b]	ND[c]
3	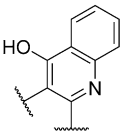	single	$<0.02\pm0$	1.8 ± 0.42	0.09 ± 0.01	4.5 ± 0.36	3.8 ± 0.36	0.04 ± 0
4	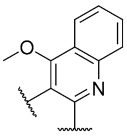	single	0.05 ± 0	12.8 ± 1.71	0.34 ± 0.03	9.5 ± 1.22	5.2 ± 0.9	ND[c]
5	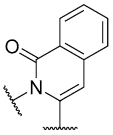	single	$<0.02\pm0$	0.43 ± 0.06	0.04 ± 0.03	1.5 ± 0.21	3.0 ± 0.05	0.05[b]
6	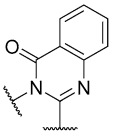	double	$<0.02\pm0$	0.6 ± 0.09	0.05 ± 0.02	0.92 ± 0.17	3.5[b]	0.08[b]
7	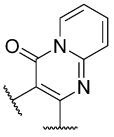	double	$<0.02\pm0$	0.5 ± 0.04	0.04 ± 0.01	2.8 ± 1.06	5.0 ± 0.02	0.06 ± 0.01
8	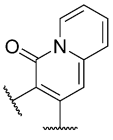	double	0.03 ± 0	0.64 ± 0.03	0.07 ± 0	2.4 ± 0	5.2 ± 0.07	ND[c]
9	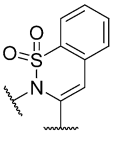	single	0.08 ± 0	47.5 ± 0.71	1.15 ± 0.21	115 ± 7.1	ND[c]	ND[c]
10		double	0.05 ± 0.01	11.0 ± 1.4	0.29 ± 0.08	7.4 ± 1.5	39.4 ± 6.1	0.45 ± 0.08

not as high as rat at 24 h, and also the dog [L]/[P] exposure ratio was only 2.8. The reason for the species difference is unknown, but might result from saturation of uptake in dog liver or species differences in tissue binding. Compound **15** displays excellent selectivity versus other serine proteases (no activity against elastase and trypsin, 176000-fold versus chymotrypsin) and against a broad Panlabs screen (>100000-fold selectivity). Given the sum of data in terms of excellent potency against gt3 and gt1 mutant enzymes, favorable preclinical PK properties, and a clean off-target profile, **15** (MK-2748) was selected for further clinical development.

During the same time that MK-2748 was being developed, we had decided to re-investigate the P1–P3/P2–P4 bis-macrocyclic series[22] to determine if, with more recently discovered P2-heterocycles, this series could also yield a compound with the potential to be an additional next-generation HCV NS3/4a protease inhibitor with a profile similar to that of MK-5172. Given the synthetic complexity inherent in this series, we decided to simplify one aspect and focus only on P2-heterocycles present in previously discovered development candidates or compounds that had already demonstrated next-generation profiles in P2–P4 mono-macrocycles (Table 4). Incorporation of the isoindoline present in MK-7009 (vaniprevir) while maintaining a related P2–P4 linker and the same P1–P3 linker as BILN-2061 leads to compound **16**, which has <5 nM potency across our standard panel of gt1b, gt3a, and gt1 mutant enzymes; however, gt1b replicon potency (7 nM) is significantly shifted in the presence of 50% NHS (58 nM) and has very poor rat liver concen-

Table 1. (Continued)

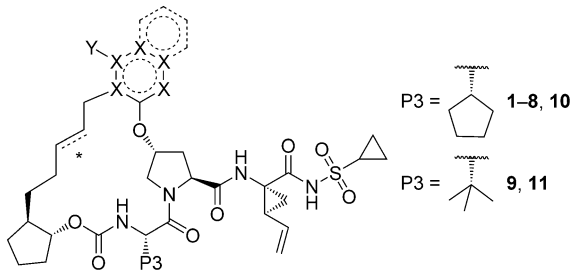

No.	P2-Heterocycle	*Bond	Enzyme Inhibition K_i [nM][a] 1b	3a	R155K	A156T	A156V	D168Y
11	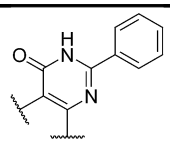	single	0.02 ± 0	2.9 ± 0.42	0.10 ± 0.01	13.5 ± 3.5	24.5 ± 2.1	ND[c]

[a] NS3/4a protease time-resolved fluorescence assay; potency values are the average ± SD of two or more iterations unless otherwise specified. [b] Single measurement. [c] Not determined.

trations at 4 h (0.2 μM) following a 5 mg kg^{-1} p.o. dose. Compound **17** has the same P2-heterocycle as MK-1220 and shows good gt1b and gt3a potency, but has much lower potency against gt1b A156T (41 nM). However, in contrast to **16**, compound **17** has a high rat liver concentration at 4 h (15.8 μM), and similar to MK-1220 itself, excellent rat plasma exposure following oral dosing (4.5 μM h at 5 mg kg^{-1}). A 2-ethoxy-7-methoxyquinoline was previously used[26,29] in an optimized P2–P4 mono-macrocyclic HCV NS3/4a inhibitor, but incorporation of the P1–P3 macrocycle in this case did not lead to significant benefit, but rather maintained a similar profile to that of the simpler mono-P2–P4 linker analogues. Next, we explored the effects of the 6-methoxyquinoxaline present in MK-5172 within the context of a bis-macrocycle (compounds **19**–**22**). Both the ring size of the cyclic constraint in the P2–P4 linker and the substitution on the cyclopropylacylsulfonamide were examined. As is evident from Table 4, all analogues dis-

Table 2. Optimization of P2-quinazolinones.

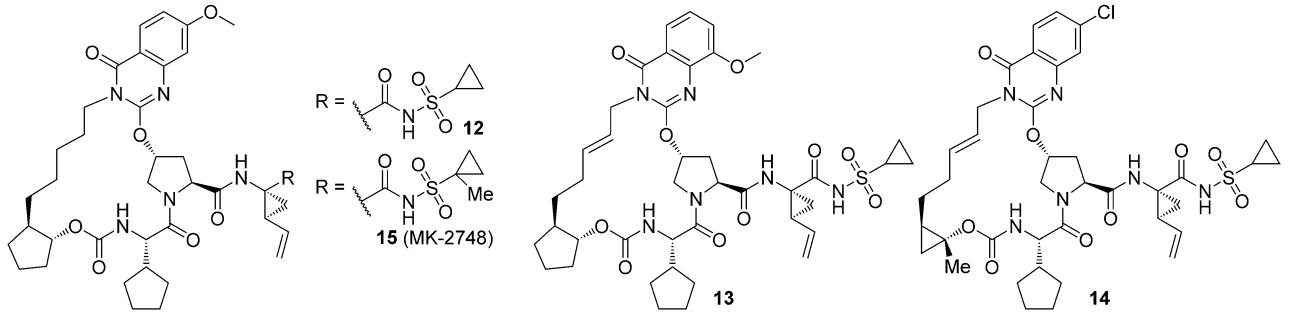

Compd	Enzyme Inhibition K_i [nM][a] 1b	3a	R155K	A156T	A156V	D168Y	gt1b EC_{50} [nM][b] 10% FBS	50% NHS	Rat PK[c] AUC_{0-4h} [μM h]	$[liver]_{4h}$ [μM]
6	< 0.02 ± 0	0.6 ± 0.09	0.05 ± 0.02	0.92 ± 0.17	3.5[d]	0.08[d]	3 ± 1.4	9 ± 0	0.04	9.0
12	< 0.02 ± 0	1.2 ± 0.68	0.06 ± 0.02	2.4 ± 1.6	7.1 ± 1.4	0.13 ± 0.02	1[d]	10[d]	0.01	41.0
13	< 0.02 ± 0	0.43 ± 0.07	0.04 ± 0.01	0.72 ± 0.12	2.85 ± 0.4	0.07 ± 0.01	9[d]	13[d]	0.03	6.0
14	0.02 ± 0	0.84 ± 0.12	0.07 ± 0	1.17 ± 0.06	1.6 ± 0.36	ND	3[d]	13[d]	< 0.01	2.7
15	0.009 ± 0.003	1.212 ± 0.296	0.032 ± 0.009	2.543 ± 0.621	2.847 ± 1.17	0.057 ± 0.014	0.8 ± 0.6	11 ± 2.2	0.7	14.0

[a] NS3/4a protease time-resolved fluorescence assay; values are the average ± SD of two or more iterations unless otherwise specified. ND: not determined. [b] Cell-based gt1b replicon assay. [c] 5 mg kg^{-1} dosed orally in PEG400 (n = 2); calculated AUC based on 4 h experiment and liver concentration after 4 h, single experiment. [d] Single measurement.

Table 3. Pharmacokinetic parameters for **15** (MK-2748).

Species	Cl_p [mL min^{-1} kg^{-1}][a]	V_d [L kg^{-1}]	$t_{1/2}$ [h][a]	F [%]	Plasma C_{max} [μM][b]	Liver C_{24h} [μM][b]	Plasma $AUC_{0-\infty}$ [μM h][b]	Liver $AUC_{0-\infty}$ [μM h][b]	[L]/[P] AUC
Rat	88 ± 67	5.0 ± 3.7	1.9 ± 0.5	~40	0.49 ± 0.04	28.9 ± 2.8	1.7	3635	2421
Dog	1.0 ± 0.2	0.12 ± 0.02	2.5 ± 0.8	27 ± 11	4.4 ± 1.9	0.28 ± 0.33	19.3 ± 19.1	46.9 ± 41.1	2.8 ± 1.7

[a] Dosing i.v.: rat (2 mg kg^{-1}, n = 3) and dog (1 mg kg^{-1}, n = 3) in 50% PEG200/DMSO. [b] Dosing p.o.: rat (5 mg kg^{-1}, n = 3) and dog (3 mg kg^{-1}, n = 3) in potassium salt, 10% Tween. Values are the average ± SD of n = 3 in a single experiment.

Table 4. Bis-macrocycles and identification of MK-6325.

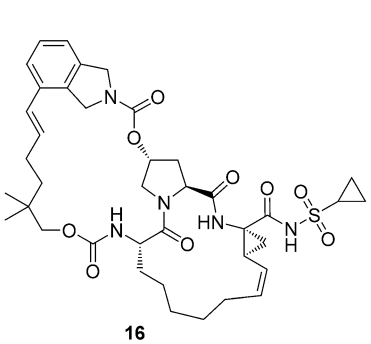

16

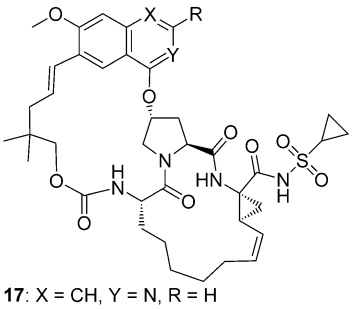

17: X = CH, Y = N, R = H
18: X = N, Y = CH, R = OEt

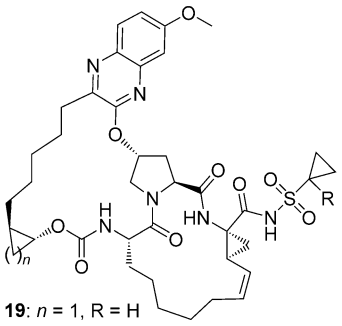

19: *n* = 1, R = H
20: *n* = 3, R = H
21: *n* = 1, R = Me
22: *n* = 3, R = Me (MK-6325)

Compd	Enzyme Inhibition K_i [nM][a]						gt1b EC_{50} [nM][b]		Rat PK[c]	
	1b	3a	R155K	A156T	A156V	D168Y	10% FBS	50% NHS	AUC_{0-4h} [μM h]	$[liver]_{4h}$ [μM]
16	0.02 ± 0.01	3.2 ± 0.62	1.35 ± 0.43	0.39[d]	2.0 ± 0.3	ND	7[d]	58[d]	0.61	0.2
17	0.04 ± 0.01	2.4 ± 0.57	0.73 ± 0.1	42 ± 11	ND	1.74 ± 0.39	2[d]	25[d]	4.5	15.8
18	0.04[d]	0.55[d]	0.16 ± 0.05	14[d]	23 ± 0	0.2[d]	2[d]	13[d]	0.03	13.5
19	< 0.02 ± 0	0.24 ± 0	0.03 ± 0.01	0.64 ± 0.13	0.85 ± 0.22	0.04 ± 0	2[d]	9[d]	0.2	6.4
20	0.16 ± 0	0.46 ± 0.03	0.07 ± 0.01	0.59 ± 0.05	1.58 ± 0.28	0.18 ± 0.02	2[d]	9[d]	< 0.01	3.6
21	0.03 ± 0	0.28 ± 0.02	0.05 ± 0.01	0.48 ± 0.11	0.63 ± 0.12	0.03 ± 0	2[d]	4[d]	0.1	19
22	0.005 ± 0.002	0.263 ± 0.107	0.013 ± 0.005	0.418 ± 0.147	0.568 ± 0.209	0.036 ± 0.014	1.1 ± 0.8	10.5 ± 3.1	0.77	43

[a] NS3/4a protease time-resolved fluorescence assay; values are the average ± SD of two or more iterations unless otherwise specified. ND: not determined. [b] Cell-based gt1b replicon assay. [c] 5 mg kg^{-1} dosed orally in PEG400 (n = 2); calculated AUC based on 4 h experiment and liver concentration after 4 h, single experiment. [d] Single measurement.

Table 5. Pharmacokinetic parameters for **22** (MK-6325).

Species	Cl_p [mL min^{-1} kg^{-1}][a]	V_d [L kg^{-1}]	$t_{1/2}$ [h][a]	F [%]	Plasma C_{max} [μM][b]	Liver C_{24h} [μM][b]	Plasma $AUC_{0-\infty}$ [μM h][b]	Liver $AUC_{0-\infty}$ [μM h][b]	[L]/[P] AUC
Rat	33 ± 18	4.0 ± 3.2	3.8 ± 1.5	~8	0.07 ± 0.04	20 ± 11	2.4	5925	2469
Dog	4.4 ± 2.0	0.5 ± 0.1	2.3 ± 0.3	12 ± 11	0.35 ± 0.30	0.12 ± 0.03	9.9 ± 4.3	27.1 ± 9.6	3.0 ± 1.6

[a] Dosing i.v.: rat (2 mg kg^{-1}, n = 3) and dog (1 mg kg^{-1}, n = 3) in 50% PEG200/DMSO. [b] Dosing p.o.: rat (5 mg kg^{-1}, n = 3) and dog (3 mg kg^{-1}, n = 3) in potassium salt, 10% Tween. Values are the average ± SD of n = 3 in a single experiment.

played superior levels of potency with < 0.5, < 0.1, and < 0.7 nM activity against gt3a, gt1b R155K, and gt1b A156T, respectively; gt1b replicon potency was also excellent, with $EC_{50} \leq$ 10.5 nM in the presence of 50% NHS for all four analogues. In contrast to their similar potency, rat PK screening data could be used to differentiate the compounds. Following a 5 mg kg^{-1} p.o. dose, rat liver concentrations at 4 h ranged from 3.6 to 43 μM, and oral exposure AUC_{0-4h} varied widely from < 0.01 to 0.77 μM h. Fortunately, the highest liver and plasma levels were provided by the same compound, **22** (MK-6325), which contains the identical cyclopentanol carbamate P2–P4 linker and methylcyclopropyl acylsulfonamide as in **15** (MK-2748).

A more detailed PK study (Table 5) showed **22** to have moderate Cl_p and V_d in rat and moderate Cl_p but low V_d in dog. In both species, **22** has low oral bioavailability (~8% in rat, 12% in dog at 5 mg kg^{-1}), but similar to **15**, rat liver exposure is maintained at a very high level for extended periods. Following a 5 mg kg^{-1} p.o. dose of the potassium salt of **22**, liver exposure at 24 h is 20 μM (> 2000-fold the 50% NHS gt1b replicon potency), whereas plasma concentrations are 0.006 nM, giving a liver/plasma ratio of > 3300. Also similar to **15**, the liver-to-plasma exposures for **22** were not as high in dog as they were in rat, which again might be attributed to saturation of uptake or species differences in tissue binding. Compound **22** also displays excellent selectivity versus other serine proteases (no activity against elastase and trypsin, 17000-fold versus chymotrypsin) and against a broad Panlabs screen (> 80000-fold selectivity). In total, based on the data in terms of gt1b, gt3a, and gt1 mutant enzyme potency along with promising preclinical PK properties and a clean off-target profile, **22** (MK-6325) was also chosen for continuation into clinical development.

To more fully assess the potential of both **15** (MK-2748) and **22** (MK-6325) as next-generation HCV NS3/4a protease inhibitors, additional profiling was carried out across a wider panel of genotypes and mutant enzymes in both biochemical and replicon assay systems (Table 6). As can be seen from Table 6A,

Table 6. Broad genotype and mutant enzyme profiling for **15** (MK-2748) and **22** (MK-6325).

A) Enzyme Inhibition IC_{50} [nM][a]			B) Replicon Potency EC_{50} [nM][b]		
Genotype	**15**	**22**	Genotype	**15**	**22**
gt1a	0.015 ± 0.004	0.011 ± 0.005	gt1a	0.5 ± 0.4	0.4 ± 0.2
gt1b	0.009 ± 0.003	0.005 ± 0.002	gt1b	0.8 ± 0.6	1.1 ± 0.8
gt2a	0.031 ± 0.010	0.014 ± 0.006	gt1a Q41R	0.8 ± 0.5	0.9 ± 0.5
gt2b	0.088 ± 0.024	0.030 ± 0.014	gt1b Q41R	1.6 ± 0.7	2.0 ± 0.5
gt3a	1.212 ± 0.296	0.263 ± 0.107	gt1b F43S	2.7 ± 1.2	3.3[c]
gt4a	0.100 ± 0.031	0.134 ± 0.111	gt1a Q80K	0.4 ± 0.2	0.6 ± 0.2
gt5a	0.115 ± 0.038	0.078 ± 0.028	gt1a R155K	0.7 ± 0.2	0.4 ± 0.3
gt6a	0.064 ± 0.026	0.045 ± 0.008	gt1b R155K	1.4 ± 0.5	1.0 ± 0.1
gt1b R155K	0.032 ± 0.009	0.013 ± 0.005	gt1b A156S	1.7 ± 0.8	0.8 ± 0.2
gt1b A156T	2.543 ± 0.621	0.418 ± 0.147	gt1b A156T	35.7 ± 9.5	5.5 ± 1.3
gt1b A156V	2.847 ± 1.170	0.568 ± 0.209	gt1a D168A	4.8 ± 1.8	1.7 ± 0.6
gt1b D168Y	0.057 ± 0.014	0.036 ± 0.014	gt1b D168A	2.6 ± 0.6	1.7 ± 0.6
			gt1b D168V	1.6 ± 0.4	2.2 ± 0.5
			gt2a	3.1 ± 1.2	4.0[c]
			gt2b	3.8 ± 0.9	2.1 ± 0.4
			gt3a	15.8 ± 7.7	4.5 ± 1.6
			gt5a	1.4 ± 0.4	2.0 ± 0.8

[a] NS3/4a protease time-resolved fluorescence assay. [b] Cell-based replicon assay. Potency values are the average ± SD of three or more iterations unless otherwise specified. [c] Single measurement.

MK-2748 maintains biochemical potency <0.115 nM across gt1–gt6, with the exception of gt3a, for which it is 1.2 nM. MK-6325 is slightly more potent, with IC_{50} values <0.263 nM across genotypes, and most being <0.1 nM. Table 6B lists the potency of MK-2748 and MK-6325 across various gt1 mutant enzymes in the replicon assay system. Similar to their enzymatic profiles, both compounds display excellent replicon potency across a panel of key gt1a (including R155K) and gt1b mutants, with all EC_{50} values <5 nM, and only one exception: gt1b A156T for MK-2748. Both compounds also display a very high level of replicon potency against non-gt1 genotypes, with MK-6325 maintaining sub-5 nM activity against gt2, gt3a, and gt5a, whereas MK-2748 also displays a similar level of potency against genotype 2a/2b ($EC_{50}<4$ nM) and gt5a ($EC_{50}=1.4$ nM) while still maintaining good gt3a potency ($EC_{50}=15.8$ nM).

Conclusions

Optimization for next-generation-like HCV NS3/4a inhibitor potency across a panel of several genotype and mutant enzymes along with selecting for compounds that provide both high liver levels and improved plasma exposure led to the discovery and development of two novel HCV NS3/4a inhibitor structural classes. Further optimization of these classes led to the identification of MK-2748 and MK-6325, the distinguishing structural features of which are a P2-quinazolinone and an 18-/15-bis-macrocyclic ring system, which along with the addition of a methyl group to the P1-cyclopropylacylsulfonamide, resulted in compounds with broad genotype and mutant potency, selectivity, and preclinical PK profile suitable for clinical development as next-generation HCV NS3/4a protease inhibitors.

Experimental Section

Compounds: Please refer to the Supporting Information for detailed synthetic procedures. All compounds were prepared and

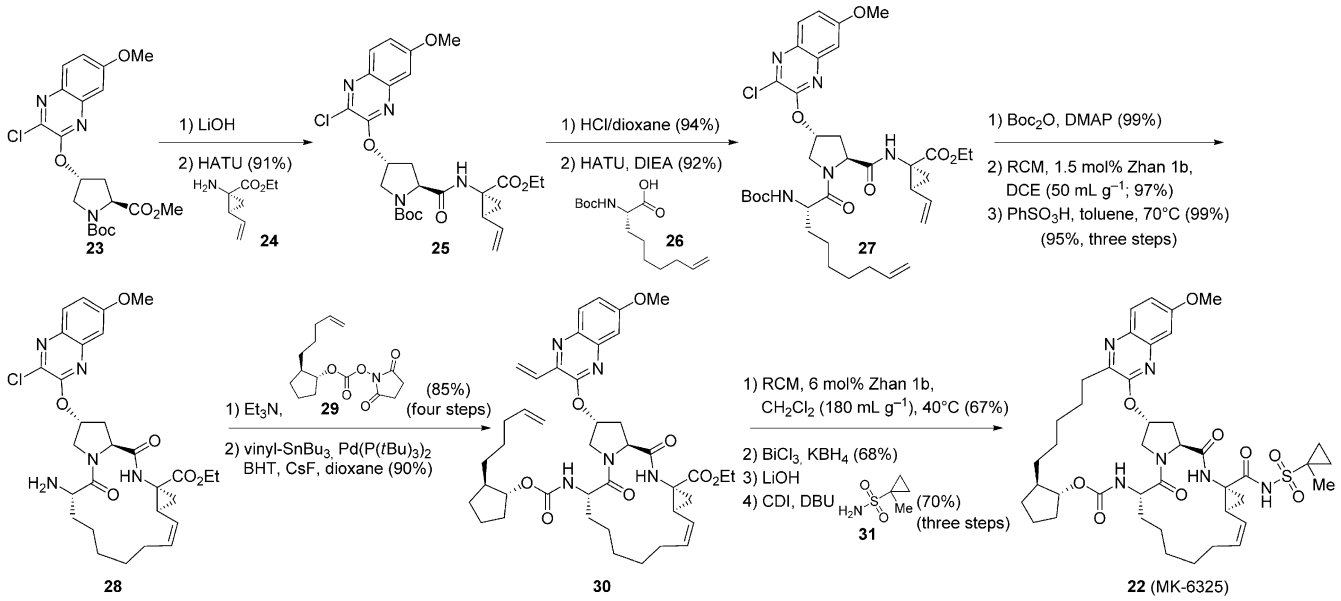

Scheme 1. Synthesis of **22** (MK-6325).

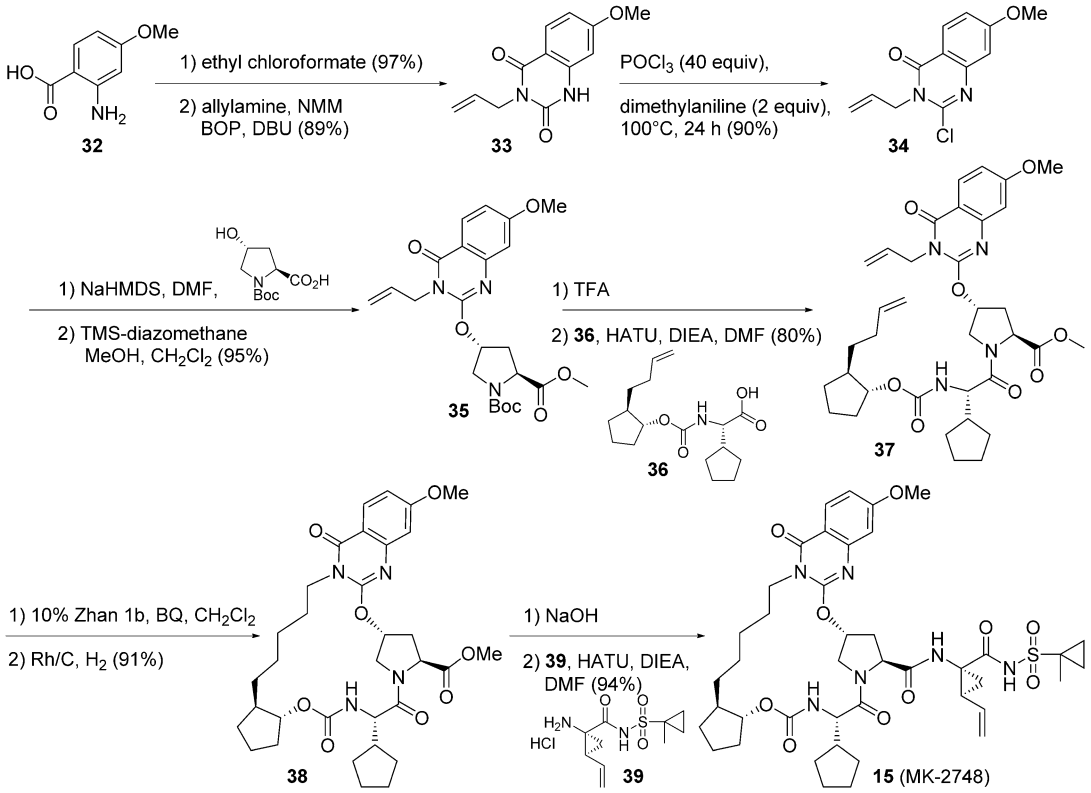

Scheme 2. Synthesis of **15** (MK-2748).

tested at >95% purity, as determined by LC–MS. Although **22** (MK-6325) could be prepared via the bis-macrocyclization sequence detailed in our previous communication,[22] in practice, the synthesis of **22** was carried out in 13 linear steps (20 total steps) by starting from (2*S*,4*R*)-1-*tert*-butyl-2-methyl-4-[(3-chloro-7-methoxyquinoxalin-2-yl)oxy]pyrrolidine-1,2-dicarboxylate (**23**), a key intermediate in the synthesis of MK-5172 (Scheme 1). Following base-mediated hydrolysis and coupling to commercially available amine **24**, the Boc group in **25** was removed, and a second amide coupling, this time to commercially available acid **26**, was carried out to yield key bis-olefin **27**. Based on the factors discovered at Boehringer Ingelheim during the development of BILN-2061,[30] we Boc-protected the amide NH group and then proceeded with the ring-closing metathesis (RCM) reaction, which, after removal of the two Boc protecting groups, yielded mono-macrocyclic amine **28** in an excellent yield of 95% over three steps as a single isomer. Addition to activated carbonate **29** and vinylation led to the second RCM precursor **30** in good yield. More dilute conditions and higher catalyst loading was required to form the desired 18-membered ring in moderate (67%) yield relative to the initial 15-membered RCM product. However, after selective reduction of the more activated styryl olefin,[31] hydrolysis, and acylsulfonamide formation with readily available sulfonamide **31**, compound **22** (MK-6325) was prepared in 18% overall yield.

Compound **15** (MK-2748) was synthesized according to a similar sequence, shown in Scheme 2. Starting from benzoic acid **32**, *N*-allylquinazolinedione **33** was prepared in 86% yield over two steps. The key cyclization precursor **37** was then synthesized after conversion into the chloroquinazolinone **34**, coupling to Boc-protected hydroxyproline, Boc deprotection, and amide formation in 68% over five steps. RCM and reduction proceeded smoothly, and following hydrolysis and another amide coupling with functionalized amine **39**, compound **15** (MK-2748) was synthesized in 50% yield over 11 linear steps.

In vitro assays: Enzymatic and replicon assays were performed as previously described.[18]

Pharmacokinetic studies: Studies were performed as previously described[18] in both rat and dog, and protocols were approved by the Merck Research Laboratory Institutional Animal Care and Use Committee.

Acknowledgements

We thank Dr. Charles W. Ross III and Ms. Joan S. Murphy for high-resolution mass spectrometry data and Sandor L. Varga for interpretation of NMR spectra.

Keywords: antiviral agents · hepatitis C · macrocycles · MK-2748 · MK-6325

[1] R. S. Brown, *Nature* **2005**, *436*, 973–978.
[2] World Health Organization, Hepatitis C Fact Sheet No. 164: who.int/mediacentre/factsheets/fs164/en/ (Last updated April 2014).
[3] J. G. McHutchison, S. C. Gordon, E. R. Schiff, M. L. Shiffman, W. M. Lee, V. K. Rustgi, Z. D. Goodman, M.-H. Ling, S. Cort, J. K. Albrecht, *N. Engl. J. Med.* **1998**, *339*, 1485–1492.
[4] M. P. Manns, J. G. McHutchison, S. C. Gordon, V. K. Rustgi, M. Shiffman, R. Reindollar, Z. D. Goodman, K. Koury, M. H. Ling, J. K. Albrecht, *Lancet* **2001**, *358*, 958–965.
[5] M. W. Fried, *Hepatology* **2002**, *36*, s237–s244.
[6] A. D. Kwong, *ACS Med. Chem. Lett.* **2014**, *5*, 214–220.

[7] J. L. Kim, K. A. Morgenstern, C. Lin, T. Fox, M. D. Dwyer, J. A. Landro, S. P. Chambers, W. Markland, C. A. Lepre, E. T. O'Malley, S. L. Harbeson, C. M. Rice, M. A. Murcko, P. R. Caron, J. A. Thomson, *Cell* **1996**, *87*, 343 – 355.
[8] K. X. Chen, F. G. Njoroge, *Curr. Opin. Investig. Drugs* **2009**, *10*, 821 – 837.
[9] D. Lamarre, P. C. Anderson, M. Bailey, P. Beaulieu, G. Bolger, P. Bonneau, M. Boes, D. R. Cameron, M. Cartier, M. G. Cordingley, A.-M. Faucher, N. Goudreau, S. H. Kawai, G. Kukolj, L. Lagace, S. R. LaPlante, H. Narjes, M.-A. Poupart, J. Rancourt, R. E. Sentjens, R. St. George, B. Simoneau, G. Steinmann, D. Thibeault, Y. S. Tsantrizos, S. M. Weldon, C.-L. Yong, M. Llinas-Brunet, *Nature* **2003**, *426*, 186 – 189.
[10] R. B. Perni, S. J. Almquist, R. A. Byrn, G. Chandorkar, P. R. Chaturvedi, L. F. Courtney, C. J. Decker, K. Dinehart, C. A. Gates, S. L. Harbeson, A. Heiser, G. Kalkeri, E. Kolaczkowski, K. Lin, Y.-P. Luong, B. G. Rao, W. P. Taylor, J. A. Thomson, R. D. Tung, Y. Wei, A. D. Kwong, C. Lin, *Antimicrob. Agents Chemother.* **2006**, *50*, 899 – 909.
[11] B. A. Malcolm, R. Liu, F. Lahser, S. Agrawal, B. Belanger, N. Butkiewicz, R. Chase, F. Gheyas, A. Hart, D. Hesk, P. Ingravallo, C. Jiang, R. Kong, J. Lu, J. Pichardo, A. Prongay, A. Skelton, X. Tong, S. Venkatraman, E. Xia, V. Girijavallabhan, F. G. Njoroge, *Antimicrob. Agents Chemother.* **2006**, *50*, 1013 – 1020.
[12] J. A. McCauley, C. J. McIntyre, M. T. Rudd, K. T. Nguyen, J. J. Romano, J. W. Butcher, K. F. Gilbert, K. J. Bush, M. K. Holloway, J. Swestock, B.-L. Wan, S. S. Carroll, J. M. DiMuzio, D. J. Graham, S. W. Ludmerer, S.-S. Mao, M. W. Stahlhut, C. M. Fandozzi, N. Trainor, D. B. Olsen, J. P. Vacca, N. J. Liverton, *J. Med. Chem.* **2010**, *53*, 2443 – 2463.
[13] N. J. Liverton, S. S. Carroll, J. Di Muzio, C. Fandozzi, D. J. Graham, D. Hazuda, M. K. Holloway, S. W. Ludmerer, J. A. McCauley, C. J. McIntyre, D. B. Olsen, M. T. Rudd, M. Stahlhut, J. P. Vacca, *Antimicrob. Agents Chemother.* **2010**, *54*, 305 – 311.
[14] Approved in Japan, October 2014.
[15] Å. Rosenquist, B. Samuelsson, P.-O. Johansson, M. D. Cummings, O. Lenz, P. Raboisson, K. Simmen, S. Vendeville, H. de Kock, M. Nilsson, A. Horvath, R. Kalmeijer, G. de la Rosa, M. Beumont-Mauviel, *J. Med. Chem.* **2014**, *57*, 1673 – 1693.
[16] T. Asselah, *Expert Opin. Pharmacother.* **2014**, *15*, 121 – 130.
[17] N. J. Liverton, M. K. Holloway, J. A. McCauley, M. T. Rudd, J. W. Butcher, S. S. Carroll, J. DiMuzio, C. Fandozzi, K. F. Gilbert, S.-S. Mao, C. J. McIntyre, K. T. Nguyen, J. J. Romano, M. Stahlhut, B.-L. Wan, D. B. Olsen, J. P. Vacca, *J. Am. Chem. Soc.* **2008**, *130*, 4607 – 4609.
[18] V. Summa, S. W. Ludmerer, J. A. McCauley, C. Fandozzi, C. Burlein, G. Claudio, P. J. Coleman, J. M. DiMuzio, M. Ferrara, M. Di Filippo, A. T. Gates, D. J. Graham, S. Harper, D. J. Hazuda, C. McHale, E. Monteagudo, V. Pucci, M. Rowley, M. T. Rudd, A. Soriano, M. W. Stahlhut, J. P. Vacca, D. B. Olsen, N. J. Liverton, S. S. Carroll, *Antimicrob. Agents Chemother.* **2012**, *56*, 4161 – 4167.
[19] S. Harper, J. A. McCauley, M. T. Rudd, M. Ferrara, M. DiFilippo, B. Crescenzi, U. Koch, A. Petrocchi, M. K. Holloway, J. W. Butcher, J. J. Romano, K. J. Bush, K. F. Gilbert, C. J. McIntyre, K. T. Nguyen, E. Nizi, S. S. Carroll, S. W. Ludmerer, C. Burlein, J. M. DiMuzio, D. J. Graham, C. M. McHale, M. W. Stahlhut, D. B. Olsen, E. Monteagudo, S. Cianetti, C. Giuliano, V. Pucci, N. Trainor, C. M. Fandozzi, M. Rowley, P. J. Coleman, J. P. Vacca, V. Summa, N. J. Liverton, *ACS Med. Chem. Lett.* **2012**, *3*, 332 – 336.
[20] C. A. Coburn, P. T. Meinke, W. Chang, C. M. Fandozzi, D. J. Graham, B. Hu, Q. Huang, S. Kargman, J. Kozlowski, R. Liu, J. A. McCauley, A. A. Nomeir, R. M. Soll, J. P. Vacca, D. Wang, H. Wu, B. Zhong, D. B. Olsen, S. W. Ludmerer, *ChemMedChem* **2013**, *8*, 1930 – 1940.
[21] S. R. Aggarwal, *Nat. Biotechnol.* **2014**, *32*, 323 – 330.
[22] J. A. McCauley, M. T. Rudd, K. T. Nguyen, C. J. McIntyre, J. J. Romano, K. J. Bush, S. L. Varga, C. W. Ross, III, S. S. Carroll, J. DiMuzio, M. W. Stahlhut, D. B. Olsen, T. A. Lyle, J. P. Vacca, N. J. Liverton, *Angew. Chem. Int. Ed.* **2008**, *47*, 9104 – 9107; *Angew. Chem.* **2008**, *120*, 9244 – 9247.
[23] K. P. Romano, A. Ali, C. Aydin, D. Soumana, A. Ozen, L. M. Deveau, C. Silver, H. Cao, A. Newton, C. J. Petropoulos, W. Huang, C. A. Schiffer, *PLoS Pathog.* **2012**, *8*, e1002832.
[24] To maintain a consistent background, the R155K mutant was screened in gt1b. The K_i values are similar for analogues for which we have data for both gt1a R155K and gt1b R155K variants.
[25] B. D. Lindenbach, C. M. Rice, *Nature* **2005**, *436*, 933 – 938.
[26] M. T. Rudd, J. A. McCauley, J. J. Romano, J. W. Butcher, K. Bush, C. J. McIntyre, K. T. Nguyen, K. F. Gilbert, T. A. Lyle, M. K. Holloway, B.-L. Wan, J. P. Vacca, V. Summa, S. Harper, M. Rowley, S. S. Carroll, C. Burlein, J. M. DiMuzio, A. Gates, D. J. Graham, Q. Huang, S. W. Ludmerer, S. McClain, C. McHale, M. Stahlhut, C. Fandozzi, A. Taylor, N. Trainor, D. B. Olsen, N. J. Liverton, *Bioorg. Med. Chem. Lett.* **2012**, *22*, 7201 – 7206.
[27] P. Raboisson, T.-I. Lin, H. de Kock, S. Vendeville, W. Van de Vreken, D. McGowan, A. Tahri, L. Hu, O. Lenz, F. Delouvroy, D. Surleraux, P. Wigerinck, M. Nilsson, A. Rosenquist, B. Samuelsson, K. Simmen, *Bioorg. Med. Chem. Lett.* **2008**, *18*, 5095 – 5100.
[28] B. Moreau, J. A. O'Meara, J. Bordeleau, M. Garneau, C. Godbout, V. Gorys, M. Leblanc, E. Villemure, P. W. White, M. Llinas-Brunet, *J. Med. Chem.* **2014**, *57*, 1770 – 1776.
[29] M. T. Rudd, C. J. McIntyre, J. J. Romano, J. W. Butcher, M. K. Holloway, K. Bush, K. T. Nguyen, K. F. Gilbert, T. A. Lyle, N. J. Liverton, B.-L. Wan, V. Summa, S. Harper, M. Rowley, J. P. Vacca, S. S. Carroll, C. Burlein, J. M. DiMuzio, A. Gates, D. J. Graham, Q. Huang, S. W. Ludmerer, S. McClain, C. McHale, M. Stahlhut, C. Fandozzi, A. Taylor, N. Trainor, D. B. Olsen, J. A. McCauley, *Bioorg. Med. Chem. Lett.* **2012**, *22*, 7207 – 7213.
[30] C. Shu, X. Zeng, M.-H. Hao, X. Wei, N. K. Yee, C. A. Busacca, Z. Han, V. Farina, C. H. Senanayake, *Org. Lett.* **2008**, *10*, 1303 – 1306.
[31] P.-D. Ren, S.-F. Pan, T.-W. Dong, S.-H. Wu, *Synth. Commun.* **1996**, *26*, 763 – 767.

Received: December 23, 2014
Published online on ■■ ▮▮, 0000

M. T. Rudd, J. W. Butcher, K. T. Nguyen, C. J. McIntyre, J. J. Romano, K. F. Gilbert, K. J. Bush, N. J. Liverton, M. K. Holloway, S. Harper, M. Ferrara, M. DiFilippo, V. Summa, J. Swestock, J. Fritzen, S. S. Carroll, C. Burlein, J. M. DiMuzio, A. Gates, D. J. Graham, Q. Huang, S. McClain, C. McHale, M. W. Stahlhut, S. Black, R. Chase, A. Soriano, C. M. Fandozzi, A. Taylor, N. Trainor, D. B. Olsen, P. J. Coleman, S. W. Ludmerer, J. A. McCauley**

■■ – ■■

P2-Quinazolinones and Bis-Macrocycles as New Templates for Next-Generation Hepatitis C Virus NS3/4a Protease Inhibitors: Discovery of MK-2748 and MK-6325

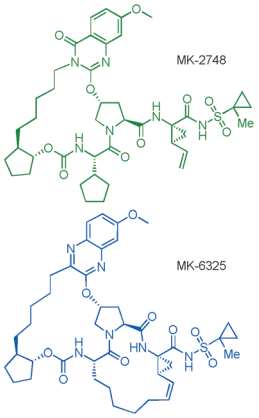

Breakthrough antivirals: We describe the discovery of two hepatitis C virus (HCV) NS3/4a protease inhibitors with excellent potency against a broad genotype and mutant range. It is anticipated that such wide-scope activity will be a prerequisite for successful clinical development of next-generation antiviral agents.